Research in Astronomy and Astrophysics, 25:045004 (10pp), 2025 April
https://doi.org/10.1088/1674-4527/adbea4
CSTR: 32081.14.RAA.adbea4

High Precision and Robust UVW Calculation for SKA1 Based on Katpoint

Yijun Xu[1], Yangfan Xie[1], Feng Wang[1], Hui Deng[1], Yin Mei[1], Johannes Allotey[2], Ying-He Celeste Lü[2], Gabriella Hodosán[3,4,5], and Oleg Smirnov[6]
[1] Center for Astrophysics and Great Bay Center of National Astronomical Data Center, Guangzhou University, Guangzhou 510006, China; fengwang@gzhu.edu.cn
[2] Cavendish Astrophysics Group, University of Cambridge, Cambridge, CB3 0HE, UK
[3] RAL Space, STFC Rutherford Appleton Laboratory, Didcot, Oxfordshire, OX11 0QX, UK
[4] Konkoly Observatory, HUN-REN Research Centre for Astronomy and Earth Sciences, Konkoly Thege Miklós út 15-17, H-1121 Budapest, Hungary
[5] CSFK, MTA Centre of Excellence, Konkoly Thege Miklós út 15-17, H-1121 Budapest, Hungary
[6] South African Radio Astronomy Observatory, Observatory 7925, South Africa
Received 2025 January 27; revised 2025 February 28; accepted 2025 March 7; published 2025 April 7

Abstract

The Square Kilometre Array (SKA) has the potential to revolutionize astronomical research through its unparalleled precision. A critical aspect of SKA imaging is the computation of the UVW coordinates, which must be accurate and reliable for the development of the SKA scientific data processor. Katpoint is the current method used to calculate UVW in MeerKAT. Using a pseudo-source, we employ a simple cross-product method to determine UVWs. In this study, we explore the applicability of Katpoint for SKA1-low and SKA1-mid and evaluate its precision. The conventional method, CALC/OmniUV, and Katpoint were quantitatively assessed through simulations. The results indicate that Katpoint exhibits substantial accuracy with MeerKAT compared to traditional techniques. However, its precision is slightly inadequate for the long baselines of SKA1. We improved the precision of Katpoint by identifying optimal offset values for pseudo-sources on the SKA1 telescope through simulation, finding a $0.^{\circ}11$ offset suitable for SKA1-Mid and a $0.^{\circ}045$ offset for SKA1-Low. Final result validations demonstrate that these adjustments render the computational accuracy fully comparable to the standard CALC/OmniUV method, which would meet the requirements of SKA high-precision imaging and offer a solution for high-precision imaging in radio interferometers.

Key words: techniques: interferometric – methods: data analysis – techniques: image processing

1. Introduction

The Square Kilometre Array (SKA) is an ultra-sensitive radio interferometer designed to better understand the most significant phenomena in the universe, including the origin and evolution of the universe (Dewdney et al. 2009). The construction of SKA1 is already underway, which combines radio astronomy interferometry techniques with modern phased array radar technology. SKA aims to improve conventional methods of radio astronomy research and open up exciting new scientific opportunities. Considering the enhanced precision and sensitivity of the antenna array, improving conventional astronomical data processing tools is also one of the goals of SKA1. Thus, high-precision, high-quality imaging processes are crucial and significant goals in SKA1 commissioning and scientific data handling.

The primary function of an interferometer is to reconstruct the brightness distribution within a specified region of the sky, often referred to as the "sky model." The visibility is mathematically represented by the equation

$$V(u, v, w) = \iint \frac{I(l, m)}{\sqrt{1 - l^2 - m^2}} \times e^{-2\pi i(ul+vm+w(\sqrt{1-l^2-m^2}-1))} dldm. \quad (1)$$

In this context, u, v, and w denote the baseline coordinates within the UVW coordinate system, while l, m, and n are the direction cosines of the observed direction, satisfying the condition ($l^2 + m^2 + n^2 = 1$).

The UVW coordinate system is crucial for processing and analyzing interferometric data, as it enables the application of the Fourier transform to convert visibility data into images of the sky. Under the requirements of high precision and high sensitivity for SKA1, computational errors should be minimized, as these errors should remain below the dynamic range threshold of SKA1. Therefore, the accuracy of UVW coordinate calculation must be correspondingly improved. Any errors in UVW calculation, such as deviations in the pointing accuracy of the W-axis, potential non-orthogonality among the UVW coordinate axes, and the U and V axes of the UV-plane not strictly pointing to the East and North, can lead to errors in the positions of corresponding visibility data on the UV-plane. These errors will directly affect subsequent imaging calculations, including the reconstruction of celestial positions and flux densities of the stars in the sky model, thereby affecting the imaging quality to varying degrees.

Each mainstream radio interferometer software, regardless of its development language, has equivalent functions to compute

UVW. The conventional approach is well documented in several renowned books (Perley et al. 1989; Taylor et al. 1999; Thompson et al. 2017) and scholarly articles. It has been implemented in numerous established software applications such as CASA (Urvashi 2013; CASA Team et al. 2022), RASCIL[7]/RASCIL2[8] (Lü et al. 2022; Xie et al. 2022, 2024), and OSKAR (Dulwich et al. 2009).

Katpoint is a well-known data processing software used by the SKA precursor telescope, MeerKAT. It is used to calculate the precise position of the observation target, and the calculation of the UV wavelength is one of its basic functions. The current implementation of the Katpoint UV-visible wavelength calculation method is simple, reliable, and fully satisfies the requirements of MeerKAT imaging calculations. During the development of the SKA Science Data Processor (SDP), Katpoint may also be used for UVW calculations. However, there has been a lack of qualitative and quantitative analysis of whether Katpoint meets the corresponding requirements of SKA.

This study provides an in-depth analysis of the precision and usability of Katpoint. Improvements are made to address the deficiencies of Katpoint. The rest of the paper is structured as follows. Section 2 provides a review of the literature on UVW calculation. In Section 3, we conduct experiments to evaluate the precision of various methods, including the conventional method, CALC/OmniUV, and Katpoint. Based on our findings, Section 4 proposes an optimal offset of the pseudo-source, as well as the impact of the position calculation library. Finally, Section 5 contains the conclusions of the study.

2. Related Work

The UVW coordinate system is a specialized framework employed in radio astronomy for describing the spatial frequencies sampled by an interferometric array. In radio interferometry, the UVW coordinates consist of three orthogonal spatial frequency components which represent the projection of physical baselines (the distances and orientations between pairs of antennas) onto a plane perpendicular to the direction of observation (refer to Figure 1(a)). UVW constitutes a right-handed coordinate system that can be derived from the Earth-Centered, Earth-Fixed (ECEF) coordinate system (Thompson et al. 2017). The component U corresponds to the spatial frequency along the East–West direction, V corresponds to the North–South direction, and W aligns with the celestial source under observation, effectively measuring the distance along the line of sight.

In radio astronomy, calculating UVW coordinates involves transforming the physical positions of the antennas from a Cartesian coordinate system, often referred to as the East-North-Up (ENU) or XYZ system, to the UVW system, which is aligned with the observation direction. The procedure typically begins with determining the antenna positions in the ENU system. These positions are then projected onto the UVW axes, defined by the hour angle (HA) and the decl. of the phase reference direction. This transformation can be mathematically expressed using direction cosines, which relate the UVW axes to the XYZ axes (Rau 2013). In addition to conventional methods mentioned above, numerous studies have introduced alternative approaches (Lanman et al. 2019; The Event Horizon Telescope Collaboration et al. 2019; Liu et al. 2022). Here, we analyze the principles of conventional methods, Katpoint and CALC/OmniUV.

2.1. Conventional Method

The conventional method for calculating UVW coordinates involves transforming the antenna coordinates from the ENU system of the reference point, along with the ENU values of each antenna, into the UVW system (Perley et al. 1989; Taylor et al. 1999; Thompson et al. 2017). This coordinate transformation is achieved through the employment of two rotation matrices, ensuring that the coordinate system remains orthogonally aligned without requiring the construction of additional auxiliary parameters. Once the UVW coordinates of each individual antenna have been determined, the UVW coordinates of the baselines are derived by computing the difference between the coordinates of each antenna pair.

The first rotation matrix transforms the antenna positions from the local ENU coordinate to the global ECEF coordinate (XYZ).

$$\begin{pmatrix} X \\ Y \\ Z \end{pmatrix} = \begin{pmatrix} -\sin(Lon) & -\sin(Lat)\cos(Lon) & \cos(Lat)\cos(Lon) \\ \cos(Lon) & -\sin(Lat)\sin(Lon) & \cos(Lat)\sin(Lon) \\ 0 & \cos(Lat) & \sin(Lat) \end{pmatrix} \times \begin{pmatrix} E \\ N \\ U \end{pmatrix} + \begin{pmatrix} X_{\mathrm{ref}} \\ Y_{\mathrm{ref}} \\ Z_{\mathrm{ref}} \end{pmatrix} \tag{2}$$

The positions of each antenna are then transformed from the ECEF coordinate system to the local UVW coordinate system. The second rotation matrix used ensures orthogonality between each pair of coordinate axes and is defined by

$$\begin{pmatrix} u \\ v \\ w \end{pmatrix} = \begin{pmatrix} \sin H_0 & \cos H_0 & 0 \\ -\sin\delta_0\cos H_0 & \sin\delta_0\sin H_0 & \cos\delta_0 \\ \cos\delta_0\cos H_0 & -\cos\delta_0\sin H_0 & \sin\delta_0 \end{pmatrix} \begin{pmatrix} X \\ Y \\ Z \end{pmatrix}, \tag{3}$$

where H_0 refers to the HA and δ_0 refers to the decl. of the phase center.

[7] https://gitlab.com/ska-telescope/external/rascil
[8] https://gitlab.com/ska-sdp-china/rascil2

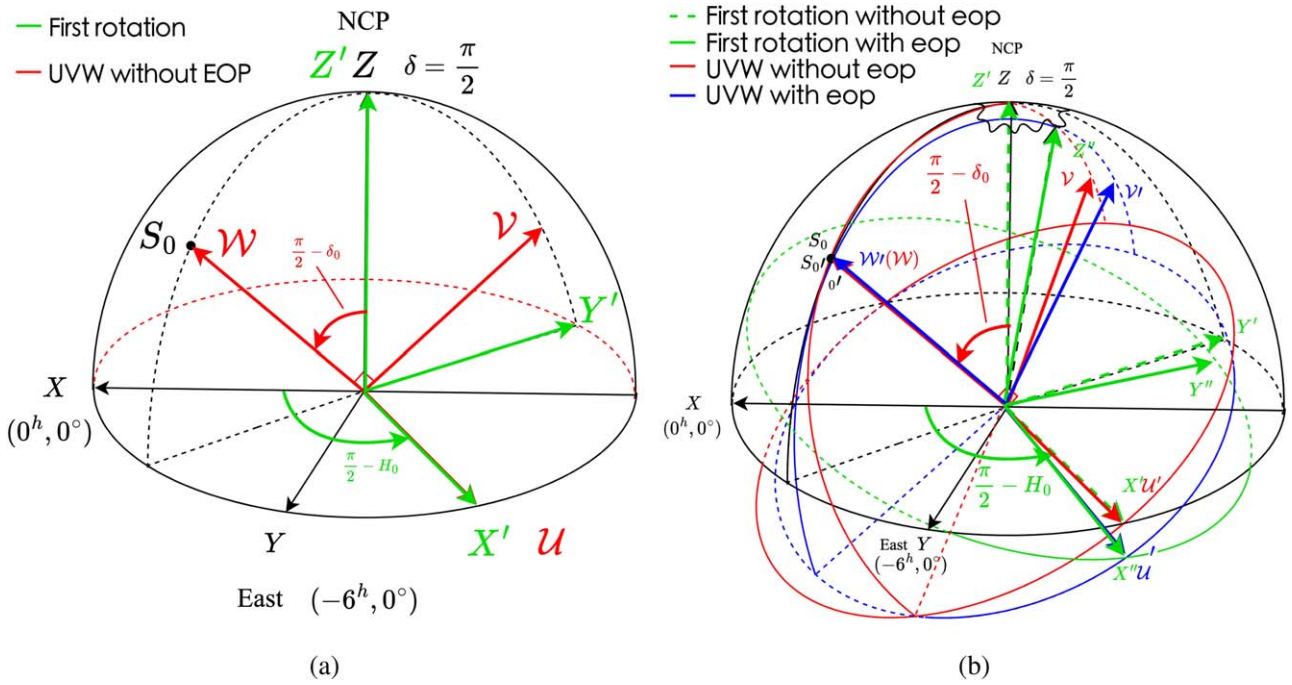

Figure 1. The diagrams for calculating UVW using the conventional method without EOP (a) and with EOP (b).

The conventional UVW calculation method, which neglects Earth Orientation Parameters (EOP), is unable to achieve high precision. After incorporating EOP, the source position shifts from the original S_0 to the adjusted S_0'. However, the conventional method fails to align the ICRS and ITRS coordinate systems, causing the U and V axes to rotate relative to the ideal UVW coordinate system (see Figure 1(b)). That is, even though the positional accuracy of the observed target is very accurate, the UVW coordinate system is not guaranteed to be parallel to the celestial sphere coordinate system, which can significantly affect the final imaging precision of the interferometers, especially for the long-baseline interferometer.

2.2. Katpoint Method

Katpoint[9] has been implemented for the MeerKAT telescope, which is the precursor array of SKA. Developed on PyEphem (Rhodes 2011), Katpoint serves as a coordinate library for the MeerKAT project. It facilitates astronomical coordinate transformations, antenna pointing models, correlator delay models, source flux models, and provides rudimentary source catalogs.

In the calculation process, Katpoint calculates UVW by creating a vector offset of 0.03 radians ($1.^\circ719$) in decl. from the observed target vector. Then it constructs the U-axis from the cross-product of these two vectors (see Figure 2).

[9] https://github.com/ska-sa/katpoint

The phase center and the pseudo-source are defined as (R.A.$_{J2000}$, decl.$_{J2000}$ − 0.03 ∗ direction_sign) in radius

$$\begin{aligned}\text{phase center} &= (\text{R.A.}_{J2000}, \text{decl.}_{J2000})\\ \text{pseudo-source} &= (\text{R.A.}_{J2000}, \text{decl.}_{J2000} - 0.03 * \text{direction\_sign})\end{aligned}. \tag{4}$$

To avoid computational issues near the poles, when constructing the offset, Katpoint sets different direction_sign in the northern and southern celestial hemispheres to ensure that the vector is closer to the celestial equator than the sources are. The direction_sign is defined as 1 when the phase center is in the northern celestial hemisphere; otherwise, it is defined as −1. It should be noted that if the target source is exactly on the equator, both calculations for the northern and southern celestial hemispheres are valid. In Katpoint and our work, the situation on the equator is treated as part of the southern celestial hemisphere for the calculation.

First, the apparent topocentric positions (az, el) of the source and pseudo-source are calculated by PyEphem (Rhodes 2011). Then, the (az, el) coordinate is transformed into an ENU coordinate by

$$\begin{aligned}E &= \sin(az) \cdot \cos(el)\\ N &= \cos(az) \cdot \cos(el)\\ U &= \sin(el).\end{aligned} \tag{5}$$

S_0 and S_1 are vectors pointing toward the phase center and the pseudo-source, respectively, in the Antenna-Centered ENU

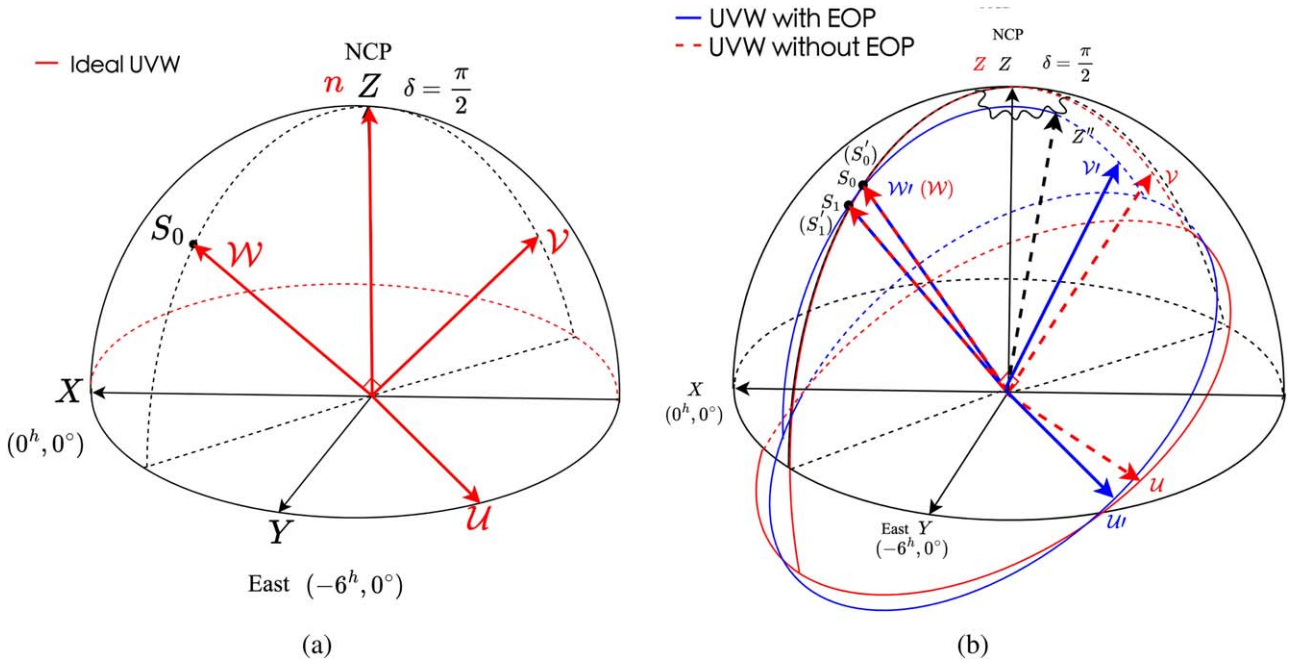

Figure 2. The diagrams for calculating UVW using Katpoint. (a) Shows the diagram for using Katpoint without EOPs. (b) Is the diagram for using Katpoint with EOP.

coordinates

$$S_0 = (E_0, N_0, U_0)$$
$$S_1 = (E_1, N_1, U_1). \quad (6)$$

e_u is the cross-product of S_0 and S_1. Finally, a set of UVW unit vectors e_v, e_w and e_u are calculated from S_0 and S_1 (see Equation (7)).

$$e_w = \frac{\boldsymbol{s}_0}{|\boldsymbol{s}_0|}$$
$$e_u = \frac{\boldsymbol{s}_1 \times \boldsymbol{s}_0}{|\boldsymbol{s}_1 \times \boldsymbol{s}_0|}$$
$$e_v = \frac{\boldsymbol{e}_w \times \boldsymbol{e}_u}{|\boldsymbol{e}_w \times \boldsymbol{e}_u|}. \quad (7)$$

The corresponding (u, v, w) of the given baseline $\boldsymbol{b}$ can be derived from the product of the baseline vector of the corresponding antenna pair and the unit vector UVW (see Equation (8)).

$$(\boldsymbol{u}, \boldsymbol{v}, \boldsymbol{w}) = \boldsymbol{b} \cdot (\boldsymbol{e_u}, \boldsymbol{e_v}, \boldsymbol{e_w}). \quad (8)$$

Overall, Katpoint has investigated methods to enhance UVW calculations. It has been implemented in the data processing of the MeerKAT telescope with highly promising results, meeting the MeerKAT imaging accuracy requirements. Despite Katpoint's successful application to MeerKAT data processing, its computational accuracy has yet to be publicly documented. It remains to be determined whether Katpoint can be seamlessly applied to SKA1-MID data processing. From the present perspective, synthesizing the advantages of various methods to explore and analyze Katpoint is evidently valuable. This will help establish the UVW calculation method capable of meeting the requirements of SKA1 and future high-precision imaging in radio interferometric arrays.

2.3. CALC/SOLVE and OmniUV

The CALC/SOLVE process is essential for VLBI data analysis, enabling precise extraction of astrometric, geodetic, and geophysical information. It compares the arrival times of radio signals at widely separated telescopes to theoretical delays based on a model that includes telescope positions, source positions, Earth's orientation, and atmospheric effects. The "CALC" step computes these delays using complex models, sometimes incorporating general relativity (Petit & Luzum 2010). The "SOLVE" step then adjusts model parameters iteratively to minimize the differences between observed and calculated delays, yielding precise positions for telescopes and sources, and EOP. The precision depends on initial model accuracy, telescope distribution, observing frequency, calibration accuracy, and systematic error modeling (Herring et al. 1990). Modern VLBI analysis, using software like VieVS (Böhm et al. 2012), achieves millimeter-level precision for stations and microarcsecond-level precision for sources, advancing geodesy, astrometry, and geophysics.

OmniUV is a simulation toolkit for VLBI observations, including lunar-based interferometers. It precisely calculates UVW parameters, crucial for describing baseline projections onto the celestial sphere. OmniUV standardizes station

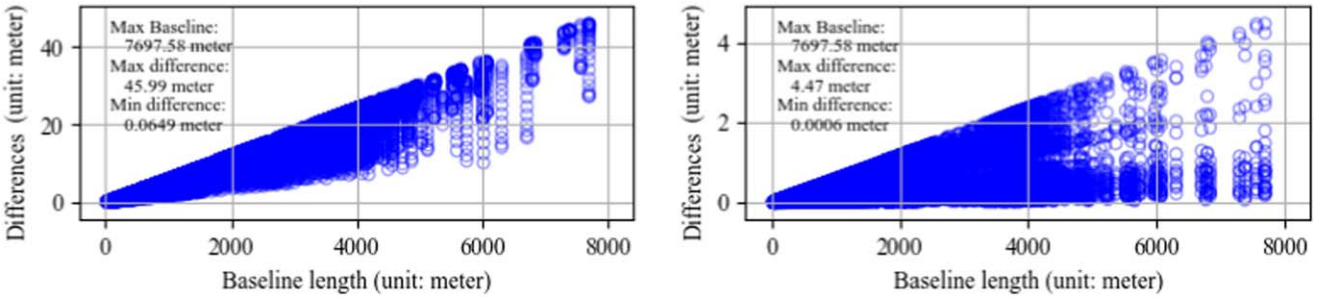

Figure 3. UVW differences between Katpoint and the conventional UVW method for MeerKAT. (a) Demonstrates the differences of UVWs calculated by the conventional method and OmniUV/CALC. (b) Shows the differences of UVW calculated by Katpoint and CALC/OmniUV.

positions into the Celestial Reference Frame (CRF) and calculates baseline vectors within this system. Like Katpoint, it uses a vector cross-product method for UVW calculations, with the target source's direction as the *W*-axis. However, while Katpoint uses a pseudo-source for the *U*-axis, OmniUV uses the North Celestial Pole (NCP). OmniUV's precision is comparable to CALC, making it highly accurate and reliable.

However, the CALC/SOLVE method is relatively complicated in implementation, requiring each antenna to be processed one by one, which does not provide high computational performance with many antennas. For radio interferometer imaging calculations where UVW calculations are needed frequently, CALC/SOLVE is not an efficient solution in such cases.

3. Precision and Usability Analyses of Katpoint

To assess the precision of Katpoint, we used several software packages for observational simulations and imaging, including RASCIL2 v1.0.0 and Katpoint v0.10. These software packages have been widely used and the results have been rigorously compared with CASA (The CASA Team et al. 2022) and WSCLEAN (Offringa et al. 2014), which are considered accurate and reliable. The test scripts were written in Python 3.10. Some dependency packages, such as Astropy 4.0 (Astropy Collaboration et al. 2013, 2018), NumPy 1.18.1, and Skyfield 1.49 (Rhodes 2019), were installed. The experimental platform is a high-end server with dual AMD 7763 CPUs (128 cores) and 2048 GB of memory. The operating system is Rocky Linux 9.0.

During the analyses, we assess the precision of the different methods by treating the results from CALC/OmniUV as the ground truth or reference values, against which all other methods are compared. For comparison, we chose Sgr A (R.A. = 266.3, decl. = 28.8055) to be used as the phase center. The observation times are 2024 April 1 03:40:59 (UTC) for the SKA1-Mid array and 2024 April 1 21:18:03 (UTC) for the SKA1-Low array. The positions of the antennas (stations) are directly quoted from the SKA design baseline and the official SKA website. It should be noted that the sources and times chosen here are only for ease of calculation and are not specific in any way.

3.1. UVW Precision Analyses for Katpoint

To investigate the precision and usability of Katpoint, two studies were carried out. One aimed to evaluate the accuracy of Katpoint in the context of MeerKAT. For this purpose, we used Katpoint and the conventional method to compute UVW for MeerKAT. The second study focused on evaluating the precision of Katpoint for calculating UVW for SKA1-Mid (Heystek 2015) and SKA1-Low (Dewdney & Braun 2016). Similarly, we calculated the UVW for SKA1-Low and SKA1-Mid using both the Katpoint and the conventional method.

Figure 3 shows that the results of the Katpoint method differ significantly from those of the conventional method. The discrepancy between the UVW results calculated by Katpoint and the conventional method increases with the length of the baseline. For the longest baseline of MeerKAT, the results calculated by Katpoint differ by nearly a factor of 10 compared to the conventional method. This difference aligns with expectations, with the EOP accounting for this variance.

3.2. Usability Analysis of Katpoint for SKA1

Furthermore, we assess the feasibility of using Katpoint for SKA1. We employ the same methodology as in the previous subsection. Katpoint and CALC/OmniUV were used to calculate the UVW for all baselines in SKA1-Low and SKA1-Mid, respectively (see Figure 4). Our findings reveal persisting discrepancies between Katpoint and OmniUV/CALC for the SKA1-Mid and SKA1-Low telescopes. Given that the longest baselines of SKA1-Low and SKA1-Mid far exceed those of MeerKAT, a discrepancy of 111.54 m is observed between Katpoint and CALC/OmniUV calculations for SKA1-Mid, and 42.25 m for SKA1-Low.

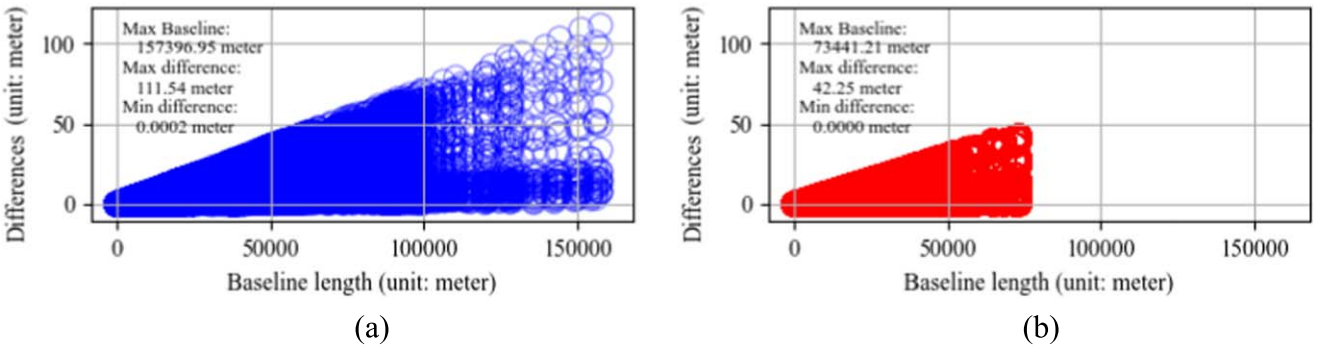

Figure 4. UVW differences between Katpoint and the CALC/OmniUV under SKA1-Mid and SKA1-Low telescope. (a): CALC/OmniUV vs. Katpoint for SKA1-Mid. (b): CALC/OmniUV vs. Katpoint for SKA1-Low.

To what extent will these discrepancies affect the final imaging? We conducted simulated observations using RASCIL2, adopting the UVW values from the CALC/OmniUV and Katpoint results. MeerKAT and SKA1-Mid were simulated at 1.1 GHz, and SKA1-Low was simulated at 125 MHz. Two sets of visibility data were obtained, with the only difference being that one set used UVW values calculated by CALC/OmniUV, while the other used values calculated by Katpoint. Each visibility was subjected to a separate imaging process, thereby allowing for a direct comparison of the resultant images. The dirty maps from the two imaging processes were subtracted to identify possible differences. Figure 5 illustrates the residual image obtained by subtracting the two dirty images.

As can be seen in the figure, the magnitude of the UVW calculation bias has a significant effect on the imaging. When the UVW calculation deviation is significant, such as comparing the results of the conventional method with those of CALC/OmniUV, it can be seen from Figure 5(b) that the residual image has an obvious peak and valley structure, indicating that there is a change in the position of the source. This difference does not arise from issues with the apparent location of the target source itself, but rather from the UVW calculation errors. In our simulations, the input target source location remains consistent in both methods; therefore, it can be recognized that these differences are entirely raised from the UVW calculation errors. In this case, we believe that UVW calculation errors introduce additional rotations in the UV-plane, causing location errors in the visibility data on the UV-plane, which in turn affect the final imaging quality. This offset is particularly significant in long-baseline observations, as these observations have higher precision requirements for UVW coordinates.

We compile the related findings from Figure 5 and present them in Table 1. The sensitivities of MeerKAT, SKA1-Low, and SKA1-Mid were calculated using SKAO's official software and documentation (see https://sensitivity-calculator.skao.int/). Differences in the flux values of point sources, labeled Flux Difference in Table 1, were recorded on various dirty maps.

For MeerKAT, the calculated Flux Difference is on the same order of magnitude as the telescope's design sensitivity. This result indicates that the calculations performed by Katpoint are sufficient to meet the imaging requirements of MeerKAT. However, the situation is different when applying the Katpoint method to SKA1-Low and SKA1-Mid. In the case of SKA1-Mid and SKA1-Low, the Flux Difference is approximately ten times greater than the telescope's sensitivity. This significant difference is entirely attributable to the UVW calculations. It can be seen that, as the baseline length increases, the computational errors of the Katpoint method become more pronounced in the imaging results, leading to a degradation in the quality of the final images. Thus, to ensure that the SKA1 project can achieve its scientific goals, it is essential to improve the Katpoint method to reduce computational errors, especially under long-baseline conditions.

4. Improve Precision of Katpoint for SKA1

Katpoint is evidently an efficient method for calculating the precise UVW coordinates of MeerKAT. It employs a rigorous mathematical approach, utilizing the cross-product of two vectors. However, what causes errors in Katpoint while using for SKA? Upon reviewing several critical aspects of the Katpoint implementation, we suspect that: (1) an offset of 0.03 radians is applied to the position of the pseudo-source in the Katpoint computation, and (2) the computation of the target source uses PyEphem. Consequently, it is worth investigating whether these elements contribute to errors in Katpoint.

4.1. Pseudo-Source Offset

To evaluate the impact of various decl. offsets of the pseudo-source on the UVW calculations and to determine the optimal values for the method, we selected a radio source and constructed a series of pseudo-sources with decl. offsets varying from $0.^{\circ}001$ to $1.^{\circ}5$, increasing by $0.^{\circ}2$ intervals, which can demonstrate the tendency of the impact without

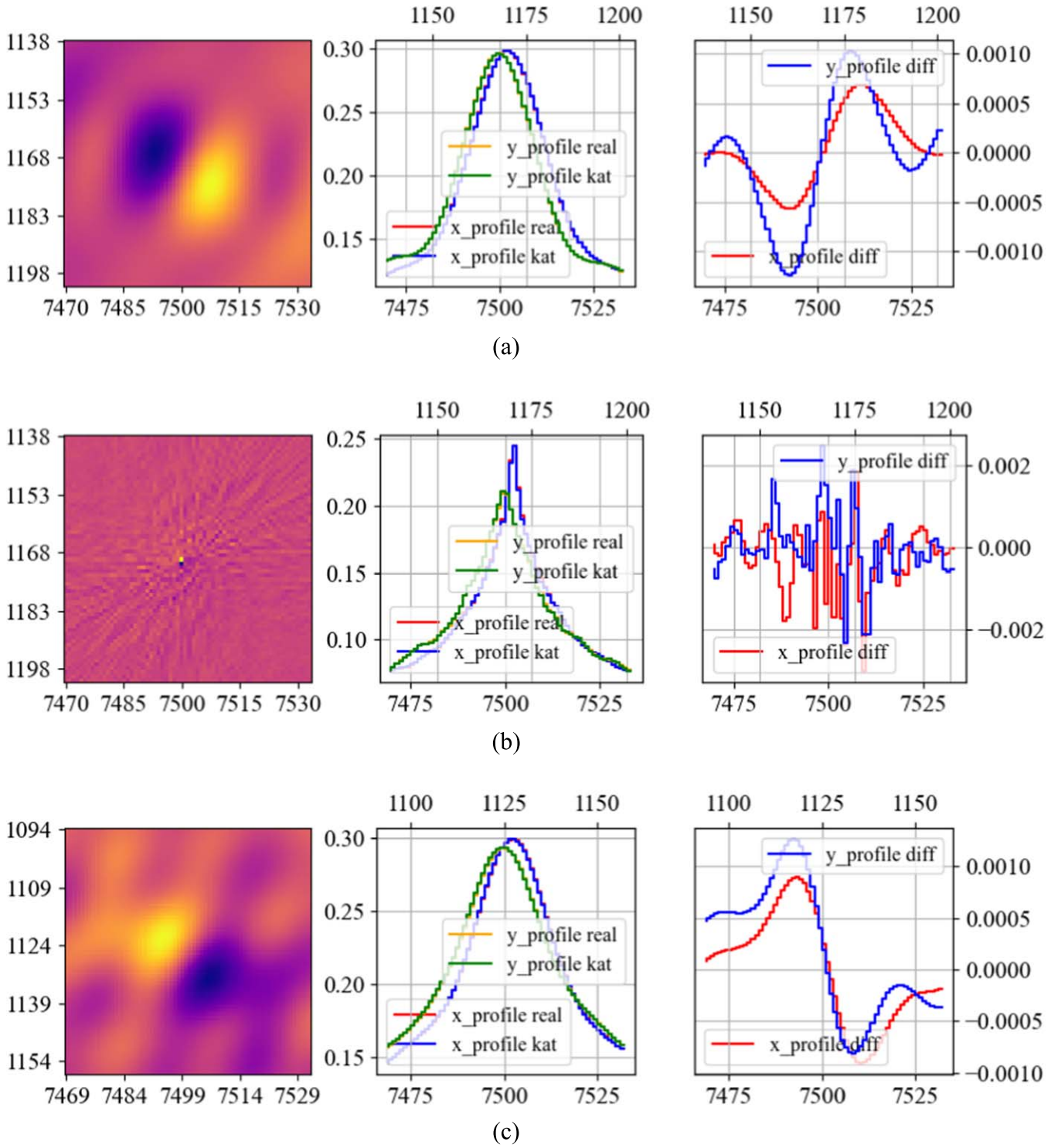

Figure 5. (a) Shows the results of two dirty images being subtracted after imaging with UVWs, calculated by the CALC/OmniUV method and Katpoint, respectively, in the MeerKAT configuration. The right two plots are the *X* vs. *Y*-axis profiling plot; (b) displays the results generated in the same way as (a) but using SKA1-Mid configuration; (c) illustrates the results generated in the same way as (a) but using SKA1-Low configuration.

Table 1
Simulation Configurations and Results

	MID	MeerKAT	LOW
Central Frequency	1.1 GHz	1.1 GHz	125 MHz
Bandwidth	2.24 MHz	2.24 MHz	9 MHz
Sensitivity (Jy beam^{-1})	2.1706e-4	8.5572e-4	1.80963e-4
Flux Difference (Jy beam^{-1})	0.002	0.001	0.001

Note. Positional differences are not listed because the phase center is the same for both imaging sessions. In this case, a different UVW calculation would only result in a rotation of the field of view.

being too dense or sparse. We then calculated the projection of these pseudo-source unit vectors onto the UV-plane (see Figure 6(a)).

It should be pointed out that the projections of the unit vectors of the pseudo-sources onto the UV-plane form a curve with increasing degrees of pseudo-source variation. This suggests that the UVW computed for pseudo-sources with different offsets is different. The root cause of this problem is that the position calculation software accurately takes into account relativistic effects and other factors during the calculation process. Specifically, the rotation of the UV-plane around the *W*-axis increases as the offset increases (see Figure 6(b)). This suggests that the offset should be minimized to prevent rotations in the field of view.

Meanwhile, due to the limitations of significant digits in computer floating-point numbers, there is indeed truncation in the storage of each vector within the computer. Consequently, if the offsets are too small, the vector cross-product may yield erroneous results. Therefore, the source offset value must not be too diminutive. This appears to be in contradiction with the smaller source offset values derived from the previous analysis.

To further determine the impact of various source offset values on intersection outcomes, we selected 299 source offset values ranging from 0.001 to 0.3 and calculated 298 intersection vectors. We evaluated the UVW computation errors and field of view rotations attributable to different source offset values for the SKA1-Mid and SKA1-Low telescopes, respectively. The results are depicted in Figure 7.

In Figure 7, it can be seen that the offset values of the source can be set at $0.^{\circ}11$ for SKA1-Mid and $0.^{\circ}045$ for SKA1-Low, which represent the optimal balance achieved by considering both rotation in the field of view and fork multiplication computational errors while ensuring sufficient accuracy. Obviously, in practice, if the longest baseline of the interferometer is longer, the value of the source offset should be relatively larger.

4.2. The Selection of Position Calculation Library

In the domain of astronomical calculations, particularly those related to the positional astronomy of celestial bodies, the libraries PyEphem (Rhodes 2011), Skyfield, and Astropy each offer distinct advantages and limitations.

PyEphem has long been a cornerstone in the field of positional astronomy, providing users with an intuitive interface for determining the positions of planets, moons, and artificial satellites. PyEphem calculates positions using the methodologies from the 1980s, as popularized in Jean Meeus's Astronomical Algorithms, employing models such as the IAU 1980 model of Earth nutation and the VSOP87 planetary theory. These enable PyEphem to be faster and more compact compared to modern astronomy libraries, yet its accuracy is limited to approximately $1''$.

In contrast, Skyfield embodies a more modern approach to astronomical computations. Designed to supersede PyEphem, it employs contemporary ephemerides, which provide improved accuracy and reliability. Its results are expected to align with the positions generated by the United States Naval Observatory and their Astronomical Almanac within $0.''0005$ (half a "mas" or milliarcsecond).

Astropy, in contrast, functions as a comprehensive framework that extends beyond simple positional calculations. It includes a wide range of functionalities, such as time management, unit conversions, and coordinate transformations. Astropy's modular design allows users to customize their experience according to specific needs, making it an invaluable tool for professional astronomers engaged in extensive data analysis. Astropy offers a flexible approach to precision by permitting users to choose from various ephemerides based on their specific requirements. This feature ensures high accuracy in calculations while also providing the extensive functionalities offered by the library. The selection of an ephemeris can significantly influence the results obtained, underscoring the importance of choosing an appropriate data set for the intended application.

Katpoint computes target locations utilizing PyEphem or Astropy. Additionally, we have incorporated Skyfield. Experiments were conducted with all three pieces of software. The experimental results demonstrate that the results from Skyfield closely align with those from CALC/OmniUV ($<10^{-12}$), and the UVW computed by Katpoint/Astropy exhibits a very small deviation from that computed by Katpoint/Skyfield, approximately 10^{-4}. Katpoint/PyEphem has the largest UVW deviation. In SKA1 imaging, the highest accuracy can be achieved by using a combination of Katpoint and Skyfield with a proper pseudo-source offset.

4.3. Empirical Assessment for the Precision of Improved Katpoint

We finally compared the precision of the improved Katpoint and the CALC/OmniUV. We selected the same radio source and the same observational time as in the previous experiments. The final results are displayed in Figure 8. Choosing the appropriate pseudo-source offsets and selecting high-precision position calculation software, the final results are essentially identical compared to those of CALC/OmniUV. The calculated UVW differences are of the order of 10^{-12}.

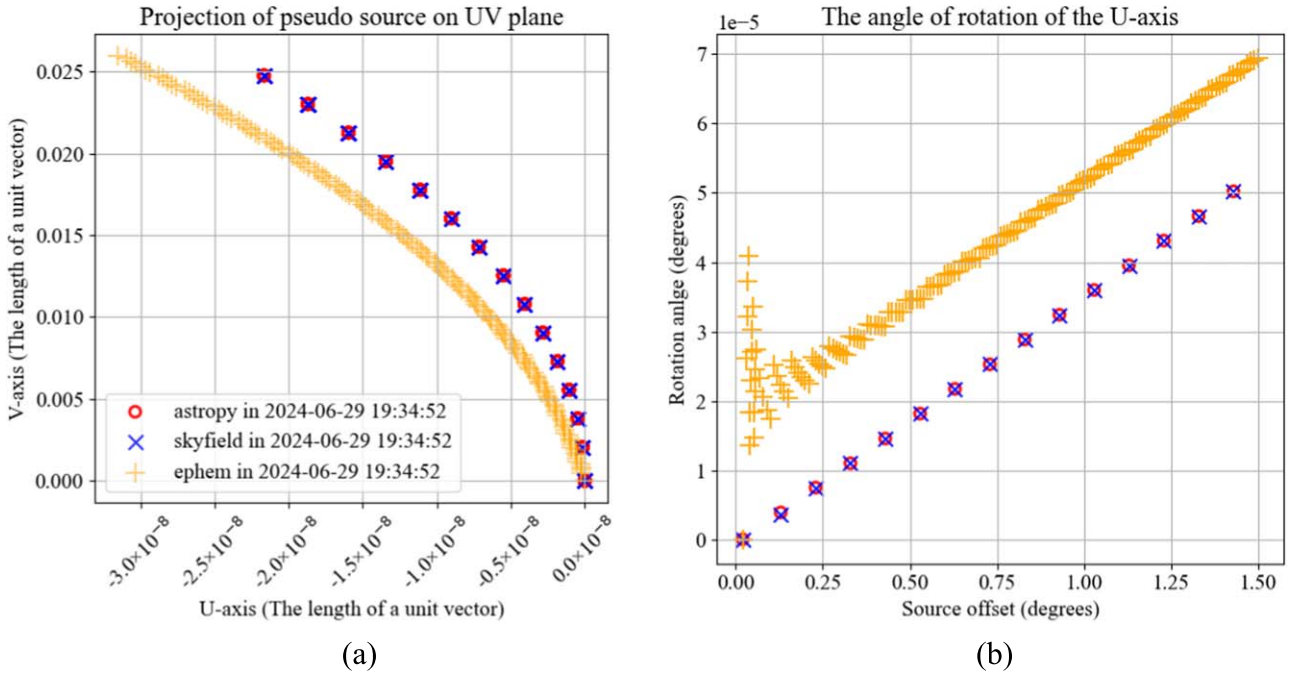

Figure 6. (a) Represents the projection of the unit vector of the pseudo-source onto the UV-plane, and (b) represents the amount of rotation of the UV-plane around the *W*-axis calculated using pseudo-sources with different offsets. Although the results calculated by PyEphem differ somewhat from those of Skyfield and Astropy, both diagrams show that the variation trend of the experimental data is the same.

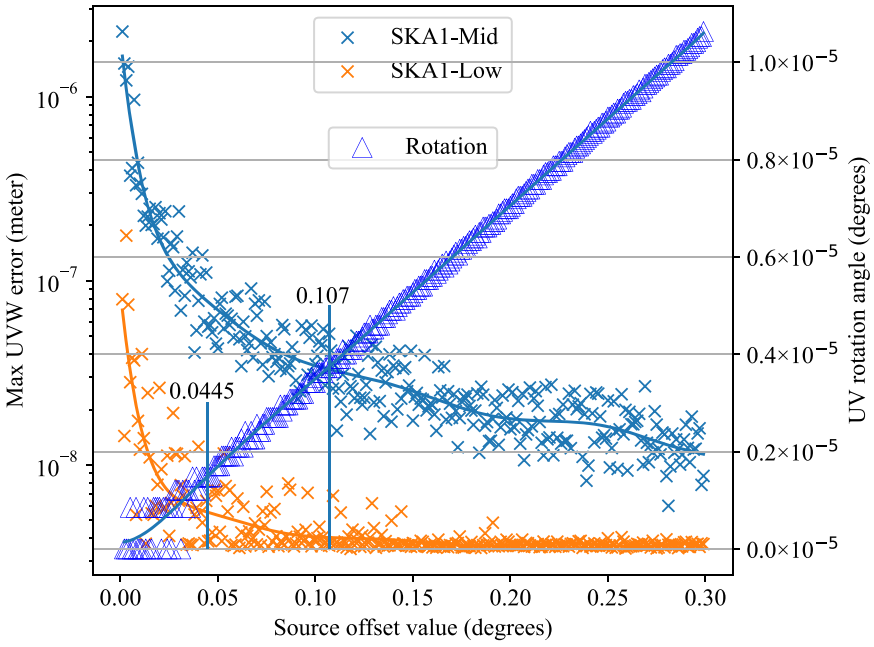

Figure 7. Comparison of UVW calculation error and UV-plane rotation angle. The vertical axis on the left has log scale, but not on the right. Therefore, the UV-plane rotation angle and source offset shown in the figure are linear.

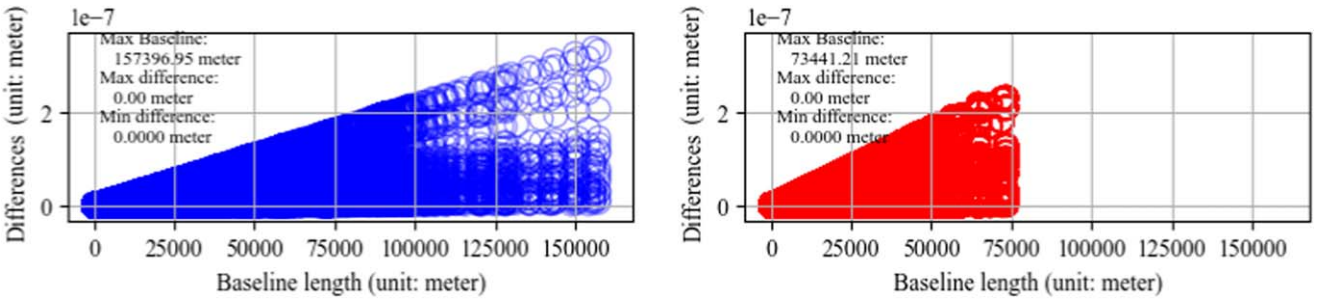

Figure 8. UVW differences between improved Katpoint and the CALC/OmniUV under SKA1-Mid (a) and improved Katpoint and the CALC/OmniUV under SKA1-Low telescope (b).

5. Conclusions and Discussions

The accuracy of UVW calculations significantly impacts subsequent data processing, particularly during the gridding process. Accurate UVW coordinate calculations are crucial for SKA1 imaging and provide the foundation for correcting various effects (such as atmospheric delay and instrumental effects), thereby ensuring the integrity of scientific conclusions drawn from SKA1 data.

We conducted an in-depth study of UVW wavelength calculations. Through experiments, we found that varying levels of precision in UVW calculations can significantly affect final imaging for specific radio interferometers, including MeerKAT, SKA1-Low, and SKA1-Mid. In particular, the longer the baseline, the greater the discrepancies between different calculation methods. From the results of the study, it is clear that the different UVW methods with the same phase center might result in a direct field of view rotation. However, if different position calculation software is used, which leads to a change in the phase center, then the effect of UVW on the imaging calculation will be reflected in two aspects: one is the translation of the whole field of view; the other is the rotation of the field of view on the basis of the translation.

In addition, we systematically analyzed the precision achievable with Katpoint and assessed its applicability to SKA1-Mid and SKA1-Low. We believe that the existing Katpoint requires further precision improvements to meet the future demands of SKA1.

Overall, we conducted a thorough analysis of Katpoint's precision issues and provided optimal solutions for the pseudo-source offset in the calculations. Ultimately, we concluded that the improved Katpoint algorithm achieves a precision comparable to CALC/OmniUV, fully satisfying the requirements for SKA imaging computations.

Acknowledgments

This work is supported by the China National SKA Programme (2020SKA0110300), the National Natural Science Foundation of China (NSFC, Grant Nos. 12433012 and 12373097), and the Guangzhou Science and Technology Funds (2023A03J0016).

Thanks to all the team members of the SKA ORCA team. Thanks to anonymous reviewers for their valuable comments.

References

Astropy Collaboration, Price-Whelan, A. M., Sipőcz, B. M., et al. 2018, AJ, 156, 123
Astropy Collaboration, Robitaille, T. P., Tollerud, E. J., et al. 2013, A&A, 558, A33
Böhm, J., Böhm, S., Nilsson, T., et al. 2012, in The New Vienna VLBI Software VieVS, International Association of Geodesy Symposia (Berlin, Heidelberg: Springer)
CASA Team, Bean, B., Bhatnagar, S., et al. 2022, PASP, 134, 114501
Dewdney, P., & Braun, R. 2016, SKA1-LOW CONFIGURATION COORDINATES COMPLETE SET, accessed: 2024-08-20
Dewdney, P. E., Hall, P. J., Schilizzi, R. T., & Lazio, T. J. L. W. 2009, IEEEP, 97, 1482
Dulwich, F., Mort, B., Salvini, S., Adami, K. Z., & Jones, M. 2009, in Proc. the Widefield Science and Technology for the SKA Conf.
Herring, T. A., Davis, J. L., & Shapiro, I. I. 1990, JGR, 95, 12561
Heystek, L. 2015, SKA1_MID PHYSICAL CONFIGURATION COORDINATES, accessed: 2024-08-20
Lanman, A. E., Hazelton, B. J., Jacobs, D. C., et al. 2019, JOSS, 4, 1234
Liu, L., Zheng, W., Fu, J., & Xu, Z. 2022, AJ, 164, 67
Lü, Y.-H. C., Hodosán, G., Wang, F., Daley-Yates, S., & Cornwell, T. 2022, in 2022 3rd URSI Atlantic and Asia Pacific Radio Science Meeting (AT-AP-RASC), 1
Offringa, A., McKinley, B., Hurley-Walker, N., et al. 2014, MNRAS, 444, 606
Perley, R. A., Schwab, F. R., Bridle, A. H. & National Radio Astronomy Observatory (U.S.) 1989, in ASP Conf. Ser. Synthesis Imaging in Radio Astronomy: A Collection of Lectures From The Third NRAO Synthesis Imaging Summer School, 6, ed. R. A. Perley (San Francisco, CA: ASP)
Petit, G., & Luzum, B. 2010, IERS Conventions (2010), Tech. Rep. 36, IERS Technical Note
Rau, U. 2013, Convention for UVW calculations in CASA, Tech. Rep., National Radio Astronomy Observatory
Rhodes, B. 2019, Skyfield: High Precision Research-grade Positions For Planets and Earth Satellites Generator, Astrophysics Source Code Library, record, ascl:1907.024
Rhodes, B. C. 2011, PyEphem: Astronomical Ephemeris for Python, Astrophysics Source Code Library, record, ascl:1112.014
Taylor, G. B., Carilli, C. L., & Perley, R. A. 1999, Synthesis Imaging in Radio Astronomy II, Synthesis Imaging in Radio Astronomy II, 180 (San Francisco, CA: ASP), 180
The CASA Team, Bean, B., Bhatnagar, S., et al. 2022, PASP, 134, 114501
The Event Horizon Telescope Collaboration, Akiyama, K., Alberdi, A., et al. 2019, ApJL, 875, L1
Thompson, A. R., Moran, J. M., & Swenson, G. W. J. 2017, Interferometry and Synthesis in Radio Astronomy, 3rd Edition (Berlin: Springer)
Urvashi, R. 2013, Convention for UVW calculations in CASA, Tech. Rep., National Radio Astronomy Observatory
Xie, Y.-F., Wang, F., Deng, H., et al. 2022, MNRAS, 515, 1973
Xie, Z., Wang, F., Mei, Y., Deng, H., & Zhu, Y. 2024, AJ, 167, 259